

---

**Research article**

## Application of sample-data control for a class of time-delay nonlinear systems in circuit systems

**Honghong Wang and Kai Wang\***

College of Electrical Engineering, Qingdao University, Qingdao 266071, China

\* **Correspondence:** Email: wangkai@qdu.edu.cn.

**Abstract:** The problem of stability and stabilization for a class of circuit systems with time-varying delays via variable period sampled-data control was considered in this paper. First, the unique boundary conditions were utilized to handle the conic-type nonlinear terms. A Lyapunov-Krasovskii (L-K) functional, which can consider both time-varying delay and sampling time information, was constructed. Then, based on the free-weighting matrices and the improved reciprocally convex combination approach, sufficient conditions for system stabilization over a wider sampling interval were obtained in terms of Linear Matrix Inequalities (LMI), enabling the determination of controller gains. Finally, considering the impact of stable operation of the circuit system on the energy consumption and life cycle of the building, a time-delayed circuit system simulation verified our results, by assuming different upper bounds on time-delay and maximum sampling intervals and designing a modal-related sampled-data controller corresponding to them. The results showed the successful application of this method in the building circuit system, which provides theoretical support for the optimization of building energy consumption and the stable operation of the circuit system.

**Keywords:** Lyapunov-Krasovskii functional; sampled-data control; time-varying delay; stability; circuit system; building energy consumption and life cycle

**Mathematics Subject Classification:** 93C10, 94A17, 62B10

---

### 1. Introduction

With the rapid development of today's society, the construction industry is facing unprecedented opportunities and challenges driven by the urbanization process and population growth [1, 2]. The energy consumption of buildings [3] not only affects its life cycle, but also has a profound impact on social, economic development and the life of people [4]. The factors that affect the energy consumption of buildings include the use of fossil fuels, the consumption of building materials and

the stable operation of the power system [5]. With the significant increase in the power load [6], the stable operation of the circuit system becomes crucial. However, the circuit system is inevitably affected by the time-delay [7] phenomenon during operation, which leads to system oscillation and instability [8]. In addition, such systems often exhibit complex nonlinear dynamic characteristics [9], and their modeling requires only dynamic boundary consideration than accurate dynamic models [10]. These factors make the life distribution [11] and reliability analysis [12] of building circuit systems a scientific problem to be solved urgently. Combined with modern statistical methods, the existing circuit model is used to analyze the various influences of its stable operation on the life distribution and reliability analysis of the building circuit system [13], and the LMI toolbox is used to analyze the system [14].

This kind of nonlinear system has been studied by more and more scholars because of its unique dynamic boundary characteristics [15]. In [16, 17], the authors discuss the existence, uniqueness, and trajectory controllability for solutions about two different stochastic differential systems. The stabilization problem of discrete nonlinear systems with perturbations is studied using the state feedback controller in [18]. The stabilization problem is studied using the sliding mode controller in [19]. The above studies provide a new idea for the stabilization of such nonlinear systems. However, it should not be ignored that the controllers used in these studies are all periodic, and few scholars use sampled-data controllers to study such nonlinear systems. The sampled-data control [20, 21] has been given more and more attention with the development of the computer hardware. Different from the traditional periodic sampling control [22], the sampled-data control adopts a non-periodic method considering the fault and jitter of the sensor [23]. In this process, many new methods have emerged, including input delay [24, 25], discrete-time model [26], and aperiodic sampled delayed measurement [27, 28]. The stability and stabilization of Markov chaotic system under fuzzy control are researched using the input delay method in [29]. The establishment of augmented functional [30] and product functional in the input delay method can consider more sampling state information and coupling relations. The synchronization problem of chaotic Lur'e systems with delay is studied using the discrete-time model method in [31]. The establishment of two-side functional [32] in the discrete-time model can consider more information of sampling time. The researchers in [33] propose a novel sampled data neural network observer to solve the problem of sampled and delayed sensor data measurements and unknown modeling uncertainties. The above different model reconstruction methods have respectively brought rich research results for sampled-data control [34]. In this research, the crossover form of these methods should be considered. Using the above ideas, it is one of our motives to explore the relationship between the maximum sampling interval and the biggest delay when the system is stabilized and to reduce conservatism.

Based on this, in this paper, the stabilization problem of time-delay nonlinear systems under sampled-data control is studied. First, the unique boundary conditions of nonlinear systems are considered to deal with nonlinear terms better; Second, a sampled-data controller is introduced to use the characteristics of time-delay systems, and a cross-type functional is constructed, which considers not only time-varying delay information, but also sampling state information and two-side sampling time information. Then, based on L-K functional [35, 36], the conditions for system stabilization are obtained, and the controller is given to obtain a big sampling interval. Finally, the simulation results show the successful application of the model in the building circuit system, which provides theoretical support for the optimization of building energy consumption and the stable operation of the circuit

system.

*Notations:* In this paper,  $\mathbb{R}^n$  and  $\mathbb{R}^{m \times n}$  denote  $n$ -dimensional vectors and  $m \times n$ -dimensional real matrices, respectively.

## 2. Problem formulation and preliminaries

Consider the nonlinear systems:

$$\begin{cases} \dot{\varsigma}(t) = A\varsigma(t) + A_d\varsigma(t - d(t)) + Bu(t) + g, \\ \varsigma(t) = v(t), -\tau \leq t \leq 0, \end{cases} \quad (2.1)$$

where  $\varsigma(t) \in \mathbb{R}^n$ ,  $u(t) \in \mathbb{R}^l$  and  $v(t)$  are the state, the controlled input, and initial condition;  $d(t)$  satisfies  $0 < d(t) < \tau$ , which is differentiable and satisfying  $\dot{d}(t) \leq \mu \leq 1$ , and  $A, A_d, B, \tau$  and  $\mu$  are known.  $g$  is a nonlinear term satisfying:

$$\|g\|^2 \leq \|L\varsigma(t) + L_d\varsigma(t - d(t))\|^2, \quad (2.2)$$

where  $L$  and  $L_d$  are known constant matrices.

By setting  $0 = t_0 < t_1 < \dots < t_r < \dots$ , we know that  $\lim_{r \rightarrow \infty} t_r = +\infty$ . Then, let  $q(t) = t - t_r$ , thus  $0 < \hat{q} \leq q(t) \leq q_r = t_{r+1} - t_r \leq \bar{q}$ ,  $\hat{q}$  and  $\bar{q}$  denote the minimum and maximum sampling intervals, respectively.

For the system (2.1), the controller of sampled-data is shown as:

$$u(t) = K\varsigma(t_r), t_r \leq t < t_{r+1}. \quad (2.3)$$

Therefore, we obtain the final system:

$$\begin{cases} \dot{\varsigma}(t) = A\varsigma(t) + A_d\varsigma(t - d(t)) + BK\varsigma(t_r) + g, \\ \varsigma(t) = v(t), t \in [-\tau, 0]. \end{cases} \quad (2.4)$$

The stable analysis and the controller design for the nonlinear system are considered in this paper.

## 3. Major results

To simplify representations of vectors and matrices, we define the following notations:

$$\begin{aligned} \xi(t) &= [\varsigma^T(t) \ \varsigma^T(t - d(t)) \ \varsigma^T(t - \tau) \ g^T \ v_1^T \ v_2^T \ \dot{\varsigma}^T(t) \ \varsigma^T(t_r) \ \varsigma^T(t_{r+1})]^T, \\ v_1 &= \int_{t-d(t)}^t \frac{\varsigma(s)}{d(t)} ds, v_2 = \int_{t-\tau}^{t-d(t)} \frac{\varsigma(s)}{\tau - d(t)} ds, e_i = [0_{n \times (i-1)n}, I_n, 0_{n \times (9-i)n}] (i = 1, 2, \dots, 9). \end{aligned} \quad (3.1)$$

Next, we give the conditions that ensure that system (2.4) is stable for the known controller gains.

**Theorem 1.** For known constants  $\tau, \mu, \hat{q}$ , and  $\bar{q}$ , matrix  $K \in \mathbb{R}^{l \times n}$ , the system (2.4) is stable for matrices  $V, S \in \mathbb{R}^{2n \times 2n}$ ,  $W_1, W_2, N_1, N_2 \in \mathbb{R}^{n \times n}$  and positive definite matrices  $U, F_1, F_2, R \in \mathbb{R}^{n \times n}$ , which satisfies the following LMIs for  $q_0 \in \{\hat{q}, \bar{q}\}$ ,  $k = 2, 3$ :

$$\begin{bmatrix} \Omega_1 + q_0 \Omega_k|_{d(t)=0} & E_1^T S \\ * & -\tilde{R} \end{bmatrix} < 0, \quad (3.2)$$

$$\begin{bmatrix} \Omega_1 + q_0 \Omega_k|_{d(t)=\tau} & E_2^T S^T \\ * & -\tilde{R} \end{bmatrix} < 0, \quad (3.3)$$

where

$$\begin{aligned} \Omega_1 &= \Phi_1 + \Phi_2 + \Phi_3 + \Phi_5 + \Phi_6 + \Upsilon_1 + \Upsilon_2, \\ \Phi_1 &= \text{sym} \{ e_1^T U e_7 \}, \Phi_2 = e_1^T (F_1 + F_2) e_1 - (1 - \mu) e_2^T F_1 e_2 - e_3^T F_2 e_3, \\ \Phi_3 &= \tau^2 e_7^T R e_7 - \begin{bmatrix} E_1 \\ E_2 \end{bmatrix}^T \begin{bmatrix} \frac{2\tau-d(t)}{\tau} \tilde{R} & S \\ * & \frac{\tau+d(t)}{\tau} \tilde{R} \end{bmatrix} \begin{bmatrix} E_1 \\ E_2 \end{bmatrix}, \\ \Phi_5 &= -(e_1 - e_8)^T W_1 (e_1 - e_8), \Phi_6 = (e_9 - e_1)^T W_2 (e_9 - e_1), \\ \Upsilon_1 &= (L e_1 + L_d e_2)^T (L e_1 + L_d e_2) - e_4^T e_4, \Upsilon_2 = \text{sym} \{ [e_7^T N_1^T + e_1^T N_2^T] [-e_7 + A e_1 + A_d e_2 + e_4 + B K e_8] \}, \\ \Omega_2 &= E_3^T V E_3 + \text{sym} \{ (e_1 - e_8)^T W_1 e_7 \}, \Omega_3 = -E_3^T V E_3 - \text{sym} \{ (e_9 - e_1)^T W_2 e_7 \}, \\ E_i &= \begin{bmatrix} e_i^T & e_{i+1}^T & e_i^T + e_{i+1}^T - 2e_{i+4}^T \end{bmatrix}, i = 1, 2, \quad E_3 = \begin{bmatrix} e_8^T & e_9^T \end{bmatrix}. \end{aligned} \quad (3.4)$$

*Proof.* Let the L-K functional as follows:

$$V(\zeta_t) = \sum_{i=1}^6 V_i(\zeta_t), \quad t_r \leq t < t_{r+1}, \quad (3.5)$$

where

$$\begin{aligned} V_1(\zeta_t) &= \zeta^T(t) U \zeta(t), \\ V_2(\zeta_t) &= \int_{t-d(t)}^t \zeta^T(s) F_1 \zeta(s) ds + \int_{t-\tau}^t \zeta^T(s) F_2 \zeta(s) ds, \\ V_3(\zeta_t) &= \tau \int_{-\tau}^0 \int_{t+u}^t \dot{\zeta}^T(s) R \dot{\zeta}(s) ds du, \\ V_4(\zeta_t) &= (t_{r+1} - t)(t - t_r) \eta^T(t) V \eta(t), \\ V_5(\zeta_t) &= (t_{r+1} - t)(\zeta(t) - \zeta(t_r))^T W_1(\zeta(t) - \zeta(t_r)), \\ V_6(\zeta_t) &= (t - t_r)(\zeta(t_{r+1}) - \zeta(t))^T W_2(\zeta(t_{r+1}) - \zeta(t)), \end{aligned}$$

where  $\eta(t) = [\zeta^T(t_r) \quad \zeta^T(t_{r+1})]^T$ .

Let  $\mathcal{L}$  be the weak-infinitesimal generator of  $(\zeta_t, t \geq 0)$ . Through calculation, we yield:

$$\mathcal{L}V_1(\zeta_t) = 2\zeta^T(t) U \dot{\zeta}(t) = \xi^T(t) \Phi_1 \xi(t), \quad (3.6)$$

$$\begin{aligned} \mathcal{L}V_2(\zeta_t) &= \zeta^T(t) F_1 \zeta(t) - (1 - d(t)) \zeta^T(t - d(t)) F_1 \zeta(t - d(t)) + \zeta^T(t) F_2 \zeta(t) - \zeta^T(t - \tau) F_2 \zeta(t - \tau) \\ &\leq \xi^T(t) \Phi_2 \xi(t), \end{aligned} \quad (3.7)$$

where  $\xi(t)$  and  $\Phi_1$  are given in (3.1) and (3.4).

Through some simple calculation to  $V_3(\zeta_t)$ , we have:

$$\mathcal{L}V_3(\zeta_t) = \tau^2 \dot{\zeta}^T(t) R \dot{\zeta}(t) - \tau \int_{t-\tau}^t \dot{\zeta}^T(u) R \dot{\zeta}(u) du. \quad (3.8)$$

Refer to Corollary 5 in [37]. The Wirtinger Integral Inequality is used to calculate the integral term of (3.8), which can be obtained as follows:

$$-\tau \int_{t-\tau}^t \dot{\zeta}^T(u) R \dot{\zeta}(u) du \leq -\frac{\tau}{d(t)} \kappa_1^T(t) \tilde{R} \kappa_1(t) - \frac{\tau}{\tau - d(t)} \kappa_2^T(t) \tilde{R} \kappa_2(t), \quad (3.9)$$

where

$$\begin{aligned} \kappa_1(t) &= \begin{bmatrix} \zeta^T(t) - \zeta^T(t-d(t)) & \zeta^T(t) + \zeta^T(t-d(t)) - 2v_1(t) \end{bmatrix}^T, \\ \kappa_2(t) &= \begin{bmatrix} \zeta^T(t-d(t)) - \zeta^T(t-\tau) & \zeta^T(t-d(t)) + \zeta^T(t-\tau) - 2v_2(t) \end{bmatrix}. \end{aligned}$$

Then, by applying Lemma 3 in [38], the Extended Reciprocally Convex Matrix Inequality is used to estimate (3.9), as follows:

$$\begin{aligned} -\frac{\tau}{d(t)} \kappa_1^T(t) \tilde{R} \kappa_1(t) - \frac{\tau}{\tau - d(t)} \kappa_2^T(t) \tilde{R} \kappa_2(t) &\leq -\begin{bmatrix} \kappa_1(t) \\ \kappa_2(t) \end{bmatrix}^T \begin{bmatrix} \frac{2\tau-d(t)}{\tau} \tilde{R} & S \\ * & \frac{\tau+d(t)}{\tau} \tilde{R} \end{bmatrix} \begin{bmatrix} \kappa_1(t) \\ \kappa_2(t) \end{bmatrix} \\ &\quad + \frac{\tau-d(t)}{\tau} \kappa_1^T(t) S \tilde{R}^{-1} S^T \kappa_1(t) + \frac{d(t)}{\tau} \kappa_2^T(t) S^T \tilde{R}^{-1} S \kappa_2(t). \end{aligned} \quad (3.10)$$

Combining (3.8)–(3.10) leads to

$$\mathcal{L}V_3(\zeta_t) \leq \xi^T(t) (\Phi_3 + \tilde{\Phi}_3) \xi(t), \quad (3.11)$$

where  $\tilde{\Phi}_3 = \frac{\tau-d(t)}{\tau} E_1^T S \tilde{R}^{-1} S^T E_1 + \frac{d(t)}{\tau} E_2^T S^T \tilde{R}^{-1} S E_2$  and  $\Phi_3$  is given in (3.4).

Through some simple calculation to  $V_4(\zeta_t)$ ,  $V_5(\zeta_t)$  and  $V_6(\zeta_t)$ , we have:

$$\mathcal{L}V_4(\zeta_t) = (t_{r+1} - t) \eta^T(t) V \eta(t) - (t - t_r) \eta^T(t) V \eta(t) = \xi^T(t) (\Phi_{41} + \Phi_{42}) \xi(t), \quad (3.12)$$

$$\begin{aligned} \mathcal{L}V_5(\zeta_t) &= -(\zeta(t) - \zeta(t_r))^T W_1 (\zeta(t) - \zeta(t_r)) + 2(t_{r+1} - t) (\zeta(t) - \zeta(t_r))^T W_1 \dot{\zeta}(t) \\ &= \xi^T(t) (\Phi_5 + \Phi_{51}) \xi(t), \end{aligned} \quad (3.13)$$

$$\begin{aligned} \mathcal{L}V_6(\zeta_t) &= (\zeta(t_{r+1}) - \zeta(t))^T W_2 (\zeta(t_{r+1}) - \zeta(t)) - 2(t - t_r) (\zeta(t_{r+1}) - \zeta(t))^T W_2 \dot{\zeta}(t) \\ &= \xi^T(t) (\Phi_6 + \Phi_{62}) \xi(t), \end{aligned} \quad (3.14)$$

where  $\Phi_5$ ,  $\Phi_6$ ,  $\Phi_{41} = (t_{r+1} - t) E_3^T V E_3$ ,  $\Phi_{42} = -(t - t_r) E_3^T V E_3$ ,  $\Phi_{51} = \text{sym}\{(t_{r+1} - t) (e_1 - e_8)^T W_1 e_7\}$  and  $\Phi_{62} = -\text{sym}\{(t - t_r) (e_9 - e_1)^T W_2 e_7\}$  are given in (3.4).

By considering the condition of nonlinearity (2.2), we can obtain:

$$0 \leq [L\zeta(t) + L_d\zeta(t-d(t))]^T [L\zeta(t) + L_d\zeta(t-d(t))] - g^T g. \quad (3.15)$$

For any  $n \times n$  matrices  $N_1^T, N_2^T$  and from the closed-loop system (2.4), we know that:

$$2 \left[ \dot{\zeta}^T(t) N_1^T + \zeta^T(t) N_2^T \right] [-\dot{\zeta}(t) + A\zeta(t) + A_d\zeta(t-d(t)) + BK\zeta(t_r) + g] = 0. \quad (3.16)$$

With the help of (3.5)–(3.16), it can be derived that:

$$\mathcal{L}V(\zeta_t) \leq \xi^T(t) \Psi \xi(t), \quad (3.17)$$

where

$$\begin{aligned}\Psi &= \Phi_1 + \Phi_2 + \Phi_3 + \tilde{\Phi}_3 + \Phi_{41} + \Phi_{42} + \Phi_5 + \Phi_{51} + \Phi_6 + \Phi_{62} + \Upsilon_1 + \Upsilon_2 \\ &= \frac{(t_{r+1} - t)}{q_r} (\Omega'_1 + q_r \Omega_2) + \frac{(t - t_r)}{q_r} (\Omega'_1 + q_r \Omega_3), \\ \Omega'_1 &= \Phi_1 + \Phi_2 + \Phi_3 + \tilde{\Phi}_3 + \Phi_5 + \Phi_6 + \Upsilon_1 + \Upsilon_2.\end{aligned}$$

Since  $\Psi$  is linear with respect to  $t$ , it can be seen from the convex combination technique that  $\Psi < 0$  is obtained if and only if  $\Psi|_{t=t_k} < 0$  and  $\Psi|_{t=t_{k+1}} < 0$ , that is:

$$\Omega'_1 + q_r \Omega_2 < 0, \quad (3.18)$$

$$\Omega'_1 + q_r \Omega_3 < 0. \quad (3.19)$$

Equations (3.18) and (3.19) are linear with respect to  $d(t)$  and  $q_r$ , respectively. Based on the convex combination technique and Schur complement, if Eqs (3.2) and (3.3) are true, then we have:

$$\Psi < 0, \quad (3.20)$$

thus,

$$\mathcal{L}V(\zeta_t) < 0. \quad (3.21)$$

Next, we show  $V(\zeta_t)$  is continuous and positive definite in time.

From (3.5), one can derive:

$$\lim_{t \rightarrow t_r} V_i(\zeta_t) = V_i(\zeta_{t_r}) \geq 0, i = 1, 2, 3, \quad (3.22)$$

$$\lim_{t \rightarrow t_r^-} V_i(\zeta_t) = \lim_{t \rightarrow t_r^+} V_i(\zeta_t) = V_i(\zeta_{t_r}) = 0, i = 4, 5, 6. \quad (3.23)$$

From (3.22) and (3.23), one has:

$$\lim_{t \rightarrow t_r} V(\zeta_t) = V(\zeta_{t_r}) \geq 0. \quad (3.24)$$

Therefore,  $V(\zeta_t)$  is continuous in time.

Moreover, from (3.21) and (3.24), we have:

$$V(\zeta_t) > V(\zeta_{t_{r+1}}) \geq 0, t_r \leq t < t_{r+1}, r = 0, 1, 2, \dots \quad (3.25)$$

which means that  $V(\zeta_t)$  is positive definite. This completes the proof.  $\square$

**Remark 1.** A set of stabilization conditions of a nonlinear system is obtained in the paper. The information of the biggest time delay and its derivatives, and the information of sampled-data and sampling time are fully considered, which reduce the conservatism greatly. Time delay  $d(t)$  and its upper bound  $\tau$  are added in  $V_2$  and  $V_3$ , and the time delay information can be taken into account more fully after derivation. The information of sampling state and two-side sampling instant is taken into account in  $V_4$  to  $V_6$ , and the integral term of sampling correlation is added. Thus the conservatism of sampling interval correlation is greatly reduced, and a larger sampling interval can be obtained.

Next, the control gain value  $K$  can be obtained for the nonlinear system (2.4) based on Theorem 1.

**Theorem 2.** For known constants  $\tau, \mu, \hat{q}, \bar{q}$  and  $\lambda$ , the system (2.4) is stable for matrices  $\bar{V}, \bar{S} \in \mathbb{R}^{2n \times 2n}, \bar{W}_1, \bar{W}_2, Y \in \mathbb{R}^{n \times n}, Z \in \mathbb{R}^{l \times n}$ , and positive definite matrices  $\bar{U}, \bar{F}_1, \bar{F}_2, \bar{R} \in \mathbb{R}^{n \times n}$ , it makes the following LMIs satisfied for  $q_0 \in \{\hat{q}, \bar{q}\}, k = 2, 3$

$$\begin{bmatrix} \bar{\Omega}_1 + q_0 \bar{\Omega}_k \Big|_{d(t)=0} & \bar{\Upsilon}_1 & E_1^T \bar{S} \\ * & -I^{n \times n} & 0 \\ * & * & -\hat{R} \end{bmatrix} < 0, \quad (3.26)$$

$$\begin{bmatrix} \bar{\Omega}_1 + q_0 \bar{\Omega}_k \Big|_{d(t)=\tau} & \bar{\Upsilon}_1 & E_2^T \bar{S}^T \\ * & -I^{n \times n} & 0 \\ * & * & -\hat{R} \end{bmatrix} < 0, \quad (3.27)$$

where

$$\begin{aligned} \bar{\Omega}_1 &= \bar{\Phi}_1 + \bar{\Phi}_2 + \bar{\Phi}_3 + \bar{\Phi}_5 + \bar{\Phi}_6 + \bar{\Upsilon}_2 - e_4^T e_4, \\ \bar{\Phi}_1 &= \text{sym} \{e_1^T \bar{U} e_7\}, \bar{\Phi}_2 = e_1^T (\bar{F}_1 + \bar{F}_2) e_1 - (1 - \mu) e_2^T \bar{F}_1 e_2 - e_3^T \bar{F}_2 e_3, \\ \bar{\Phi}_3 &= \tau^2 e_7^T \bar{R} e_7 - \begin{bmatrix} E_1 \\ E_2 \end{bmatrix}^T \begin{bmatrix} \frac{2\tau-d(t)}{\tau} \hat{R} & S \\ * & \frac{\tau+d(t)}{\tau} \hat{R} \end{bmatrix} \begin{bmatrix} E_1 \\ E_2 \end{bmatrix}, \hat{R} = \begin{bmatrix} \bar{R} & 0 \\ 0 & 3\bar{R} \end{bmatrix}, \\ \bar{\Phi}_5 &= -(e_1 - e_8)^T \bar{W}_1 (e_1 - e_8), \bar{\Phi}_6 = (e_9 - e_1)^T \bar{W}_2 (e_9 - e_1), \\ \bar{\Upsilon}_1 &= LY e_1 + L_d Y e_2, \bar{\Upsilon}_2 = \text{sym} \{[e_7^T + \lambda e_1^T] [-Ye_7 + AYe_1 + A_d Ye_2 + e_4 + BZe_8]\}, \\ \bar{\Omega}_2 &= E_3^T \bar{V} E_3 + \text{sym} \{(e_1 - e_8)^T \bar{W}_1 e_7\}, \bar{\Omega}_3 = -E_3^T \bar{V} E_3 - \text{sym} \{(e_9 - e_1)^T \bar{W}_2 e_7\}. \end{aligned} \quad (3.28)$$

Moreover, we can obtain  $K = ZY^{-1}$ .

*Proof.* Define  $N_1 = Y^{-1}, N_2 = \lambda Y^{-1}, Z = KY, \bar{U} = Y^T UY, \bar{F}_1 = Y^T F_1 Y, \bar{F}_2 = Y^T F_2 Y, \bar{R} = Y^T RY, \bar{W}_1 = Y^T W_1 Y, \bar{W}_2 = Y^T W_2 Y, \hat{R} = Y_2^T \tilde{R} Y_2, \bar{S} = Y_2^T S Y_2, \bar{V} = Y_2^T V Y_2, \mathcal{Y} = \text{diag} \{Y_3^T, I, Y_2^T, Y_3^T, Y_2^T\}$ , where  $Y_2 = \text{diag} \{Y, Y\}, Y_3 = \text{diag} \{Y, Y, Y\}$ .

Now, pre and post multiplying (3.2)-(3.3) with its transpose, yields the following inequation:

$$\begin{bmatrix} \bar{\Omega}_1 + q_0 \bar{\Omega}_k \Big|_{d(t)=0} & \bar{\Upsilon}_1^T \bar{\Upsilon}_1 & E_1^T \bar{S} \\ * & -\hat{R} & \end{bmatrix} < 0, \quad (3.29)$$

$$\begin{bmatrix} \bar{\Omega}_1 + q_0 \bar{\Omega}_k \Big|_{d(t)=\tau} & \bar{\Upsilon}_1^T \bar{\Upsilon}_1 & E_2^T \bar{S}^T \\ * & -\hat{R} & \end{bmatrix} < 0. \quad (3.30)$$

Based on the Schur complement, if (3.26)-(3.27) are satisfied, (3.29)-(3.30) are satisfied too. This completes the proof.  $\square$

**Remark 2.** To verify the effect of adding two-side sampling time information for reducing the correlation conservatism of the sampling interval, on the basis of Theorem 1 and 2, the functional is removed, and we get Corollary 1.

**Corollary 1.** For known constants  $\tau, \mu, \hat{q}, \bar{q}$ , and  $\lambda$ , the system (2.4) is stable for matrices  $\bar{W}_1, \bar{W}_2, Y \in \mathbb{R}^{n \times n}, \bar{S} \in \mathbb{R}^{2n \times 2n}, Z \in \mathbb{R}^{l \times n}$ , and positive definite matrices  $\bar{U}, \bar{F}_1, \bar{F}_2, \bar{R} \in \mathbb{R}^{n \times n}$ , satisfying the following

LMIs for  $q_0 \in \{\hat{q}, \bar{q}\}$ ,  $k = 2, 3$ :

$$\begin{bmatrix} \bar{\Omega}_1 + q_0 \tilde{\Omega}_k \Big|_{d(t)=0} & \bar{\Upsilon}_1 & E_1^T \bar{S} \\ * & -I^{n \times n} & 0 \\ * & * & -\hat{R} \end{bmatrix} < 0, \quad (3.31)$$

$$\begin{bmatrix} \bar{\Omega}_1 + q_0 \tilde{\Omega}_k \Big|_{d(t)=\tau} & \bar{\Upsilon}_1 & E_2^T \bar{S}^T \\ * & -I^{n \times n} & 0 \\ * & * & -\hat{R} \end{bmatrix} < 0, \quad (3.32)$$

where

$$\tilde{\Omega}_2 = \text{sym} \{ (e_1 - e_8)^T \bar{W}_1 e_7 \}, \tilde{\Omega}_3 = -\text{sym} \{ (e_9 - e_1)^T \bar{W}_2 e_7 \}. \quad (3.33)$$

#### 4. A numerical example

Consider a circuit system (2.4) with the following parameters [19]:

$$A = \begin{bmatrix} -8.36 & 6.5 & 0 \\ 1 & -1 & 1 \\ 0 & -11.75 & 0 \end{bmatrix}, Ad = \begin{bmatrix} -0.5 & 0 & 0 \\ -0.5 & 0 & 0 \\ 1 & 0 & -0.5 \end{bmatrix}, D = \begin{bmatrix} 6.5 & 0 & 0 \\ 0 & 0 & 0 \\ 0 & 0 & 0 \end{bmatrix}, L = \begin{bmatrix} 0.43 & 0 & 0 \\ 0 & 0 & 0 \\ 0 & 0 & 0 \end{bmatrix},$$

$$Ld = 0, g = \begin{bmatrix} f^T(\varsigma_1(t)) & 0 & 0 \end{bmatrix}^T, B = \begin{bmatrix} -0.72 & -1.5 & 0.1 \end{bmatrix}^T.$$

where  $f(\varsigma_1(t)) = 0.43 [| \varsigma_1 + E | - | \varsigma_1 - E |] / 2$ .

For given  $\lambda = 3.3$ ,  $\hat{q} = 10^{-4}$ , various  $\mu$  and  $\tau$ , the  $\bar{q}$  is obtained by Theorem 2 and Corollary 1 in Table 1. The following conclusions can be drawn: When  $\mu = 0$ ,  $\tau \geq 0.64$ , with the increase of  $\tau$ , the value of  $\bar{q}$  hardly changes anymore, indicating that no matter how large the time delay is, an appropriate sampled-data controller gain and the value of  $\bar{q}$  always can be found to stabilize the system. When  $\mu = 1$ , with the increase of  $\tau$ , the value of  $\bar{q}$  gradually decreases until there is no solution, indicating that there is an upper limit of  $\tau$  that can stabilize the nonlinear system. When  $\tau$  is less than this critical value, the controller can stabilize the nonlinear system.

**Table 1.** The maximum sampling interval  $\bar{q}$ .

$\hat{q} = 10^{-4}, \mu = 0$						$\hat{q} = 10^{-4}, \mu = 1$			
$\tau$	0.3	0.31	0.45	0.64	100	0.3	0.31	1.5	3.7
Theorem 2 $\bar{q}$	—	0.3564	0.2610	0.2199	0.2187	—	0.5565	0.1245	0.0015
Corollary 1 $\bar{q}$	—	0.2870	0.2292	0.1960	0.1945	—	0.2870	0.1108	0.0013

On this basis, the biggest time-delay  $\tau$ , for various  $\mu$  and  $\bar{q}$  is obtained by Theorem 2 in Table 2. The data in Table 2 also verifies the accuracy of the conclusions obtained in Table 1.

**Table 2.** The upper bounds on time-delay  $\tau$ .

$\hat{q} = 10^{-4}, \mu = 0$						$\hat{q} = 10^{-4}, \mu = 1$			
$\bar{q}$	0.21	0.22	0.3	0.36	100	$10^{-4}$	0.22	0.36	100
Theorem 2 $\tau$	—	0.6381	0.3724	0.3082	0.3014	3.7343	0.5893	0.3082	0.3015

**Remark 3.** Both Theorem and Corollary are given in the form of LMI. Considering that it is difficult to solve the uncertain scalar polarity when solving LMI, in order to accurately solve the two values of  $\tau$  and  $\bar{q}$ , one parameter is fixed first, and then dichotomy is used to solve quickly. For details about the value selection rule, see Remark 4.

**Remark 4.** In Table 1, when  $\tau \leq 0.3$ , the value of  $\bar{q}$  is very large, so 0.3 and 0.31 are selected for the first and second value; as  $\tau$  increases, the value of  $\bar{q}$  hardly changes, so the fifth value is 100. Similarly in Table 2, 0.21 and 0.22 are selected for the first and second value, and the fifth value is 100. The fourth value in Table 1 corresponds to the value of  $\tau$  when  $\bar{q} = 0.22$  in Table 2; furthermore, the fourth value in Table 2 corresponds to the value when  $\tau = 0.31$  in Table 1. These two values represent the limit value under this condition and are representative. The third values in Tables 1 and 2 are the intermediate values in this case.

**Remark 5.** In addition to that, according to Table 1, under the same conditions, the data obtained from Theorem 2 are always bigger than the data obtained from Corollary 1, indicating that Theorem 2 exhibits lower conservatism and demonstrates the superiority of the two-sided looped L-K functional.

Given the initial value  $\zeta(0) = [0.5 \ 0.3 \ 0.1]^T$ , sampling and time-delay related parameters  $\bar{q} = 0.2, d(t) = 1, \lambda = 1.7$ , by solving the LMIs (3.26)-(3.27), the gain is  $K = [-0.3312 \ -1.5488 \ -0.3585]$ . The state trajectories with and without controller and the controller trajectories are shown in Figures 1–3.

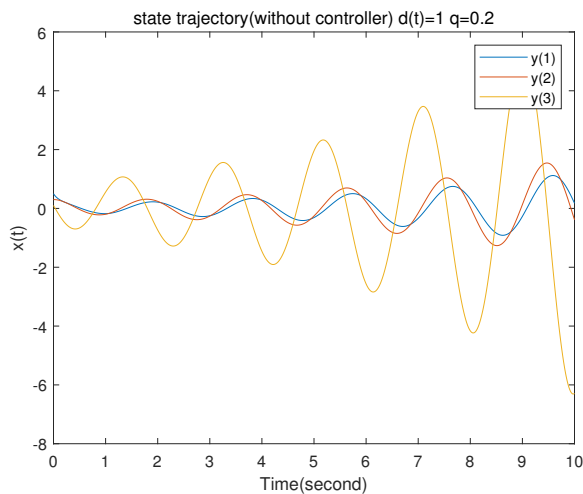


**Figure 1.** The state trajectories without the controller.

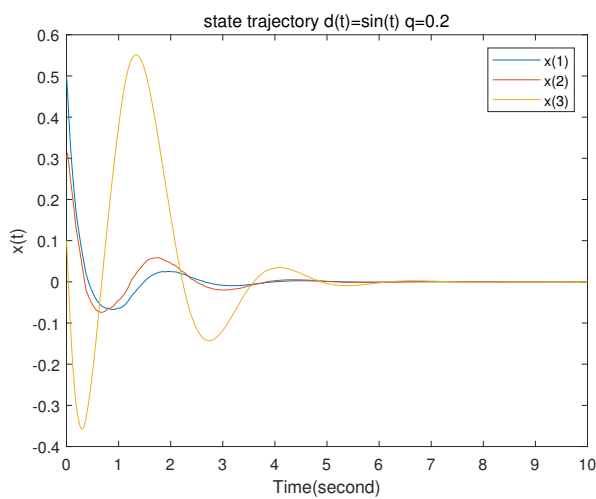


**Figure 2.** The state trajectories with the controller.

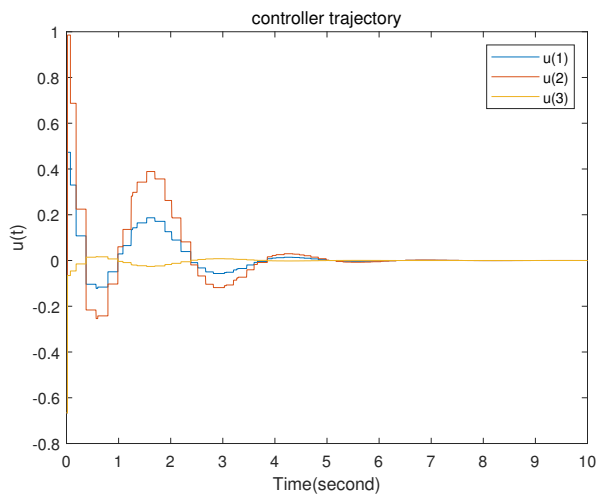


**Figure 3.** The controller trajectories.

## 5. Conclusions

The stabilization problem of a nonlinear system with time delay has been discussed by employing the L-K functional method. By designing sampled-data controller, we establish a delay-dependent and sampled-data-dependent L-K functional, whose derivative is handled by integral inequality and matrix inequality. Then, a sufficient criterion for the stabilization of nonlinear system and the controller gain has been obtained in terms of LMIs. Finally, considering the problem that the unstable operation of the circuit system has an adverse effect on the energy consumption and life cycle of the building, a circuit system example is selected and used to verify that the proposed method can make the circuit system in the building run stably and make a favorable contribution to the energy consumption and life cycle of the building. In the future, we plan to address the design problem of sampled-data controller for nonlinear systems with time-varying delays.

## Author contributions

All authors contributed to the study conception and design. The first manuscript was written by Honghong Wang. Kai Wang provided guidance and comments on the manuscript. All authors have read and approved the final version of the manuscript for publication.

## Use of Generative-AI tools declaration

The authors declare they have not used Artificial Intelligence (AI) tools in the creation of this article.

## Acknowledgments

This work was supported by the first batch of key projects in Shandong Province's marine service industry in 2025.

## Conflict of interest

The authors declare no conflicts of interest.

## References

1. Y. Pan, K. Xu, R. Wang, H. Wang, G. Chen, K. Wang, Lithium-ion battery condition monitoring: a frontier in acoustic sensing technology, *Energies*, **18** (2025), 1068. <https://doi.org/10.3390/en18051068>
2. N. Cao, H. Du, J. Lu, Z. Li, Q. Qiang, H. Lu, Designing ionic liquid electrolytes for a rigid and Li<sup>+</sup>-conductive solid electrolyte interface in high performance lithium metal batteries, *Chem. Phys. Lett.*, **866** (2025), 141959. <https://doi.org/10.1016/j.cplett.2025.141959>
3. M. Ilbeigi, M. Ghomeishi, A. Dehghanbanadaki. Prediction and optimization of energy consumption in an office building using artificial neural network and a genetic algorithm, *Sustain. Cities Soc.*, **61** (2020), 102325. <https://doi.org/10.1016/j.scs.2020.102325>
4. L. Kang, B. Xu, P. Li, K. Wang, J. Chen, H. Du, et al., Controllable preparation of low-cost coal gangue-based SAPO-5 molecular sieve and its adsorption performance for heavy metal ions, *Nanomaterials*, **15** (2025), 366. <https://doi.org/10.3390/nano15050366>
5. H. Zhang, Z. Li, Y. Liu, X. Du, Y. Gao, W. Xie, et al., Oxygen vacancies-modulated C –  $WO_3$ /BiOBr heterojunction for highly efficient benzene degradation, *Vacuum*, **234** (2025), 114117. <https://doi.org/10.1016/j.vacuum.2025.114117>
6. D. Xu, L. Zhang, H. Wang, K. Wang, W. Zhang, An investigation of the ventilation systems of whole-indoor urban substations, *Buildings*, **14** (2024), 3749. <https://doi.org/10.3390/buildings14123749>
7. Q. Zhu, Event-triggered sampling problem for exponential stability of stochastic nonlinear delay systems driven by Lévy processes, *IEEE Trans. Automat. Control*, **70** (2025), 1176–1183. <https://doi.org/10.1109/TAC.2024.3448128>

8. J. Sun, G. Han, Z. Zeng, Y. Wang, Memristor-based neural network circuit of full-function pavlov associative memory with time delay and variable learning rate, *IEEE Trans. Cybern.*, **50** (2020), 2935–2945. <https://doi.org/10.1109/TCYB.2019.2951520>
9. Q. Zhu, Stabilization of stochastic nonlinear delay systems with exogenous disturbances and the event-triggered feedback control, *IEEE Trans. Automat. Control*, **64** (2019), 3764–3771. <https://doi.org/10.1109/TAC.2018.2882067>
10. X. M. Zhang, Q. L. Han, X. Ge, A novel approach to  $H_\infty$  performance analysis of discrete-time networked systems subject to network-induced delays and malicious packet dropouts, *Automatica*, **136** (2022), 110010. <https://doi.org/10.1016/j.automatica.2021.110010>
11. Y. Zheng, Z. Y. Dong, Y. Xu, K. Meng, J. H. Zhao, J. Qiu, Electric vehicle battery charging/swap stations in distribution systems: comparison study and optimal planning, *IEEE Trans. Power Syst.*, **29** (2014), 221–229. <https://doi.org/10.1109/TPWRS.2013.2278852>
12. Y. Pan, K. Xu, Z. Chen, K. Wang, Advanced techniques for internal temperature monitoring in lithium-ion batteries: a review of recent developments, *Coatings*, **15** (2025), 268. <https://doi.org/10.3390/coatings15030268>
13. Y. Chen, Z. Zhang, B. Yang, B. Zhang, L. Fu, Z. He, A clamp circuit-based inductive power transfer system with reconfigurable rectifier tolerating extensive coupling variations, *IEEE Trans. Power Electron.*, **39** (2024), 1942–1946. <https://doi.org/10.1109/TPEL.2023.3303487>
14. S. R. Jia, W. J. Lin, Adaptive event-triggered reachable set control for Markov jump cyber-physical systems with time-varying delays, *AIMS Math.*, **9** (2024), 25127–25144. <https://doi.org/10.3934/math.20241225>
15. C. Qin, W. J. Lin, Adaptive event-triggered fault-tolerant control for Markov jump nonlinear systems with time-varying delays and multiple faults, *Commun. Nonlinear Sci. Numer. Simul.*, **28** (2024), 107655. <https://doi.org/10.1016/j.cnsns.2023.107655>
16. D. Chalishajar, D. Kasinathan, R. Kasinathan, R. Kasinathan, Exponential stability, T-controllability and optimal controllability of higher-order fractional neutral stochastic differential equation via integral contractor, *Chaos, Soliton. Fract.*, **186** (2024), 115278. <https://doi.org/10.1016/j.chaos.2024.115278>
17. D. Chalishajar, D. Kasinathan, R. Kasinathan, R. Kasinathan, Viscoelastic Kelvin–Voigt model on Ulam–Hyer’s stability and T-controllability for a coupled integro fractional stochastic systems with integral boundary conditions via integral contractors. *Chaos, Soliton. Fract.*, **191** (2025), 115785. <https://doi.org/10.1016/j.chaos.2024.115785>
18. M. N. ElBsat, E. E. Yaz, Robust and resilient finite-time bounded control of discrete-time uncertain nonlinear systems, *Automatica*, **49** (2013), 2292–2296. <https://doi.org/10.1016/j.automatica.2013.04.003>
19. R. Nie, S. He, F. Liu, X. Luan, Sliding mode controller design for conic-type nonlinear semi-Markovian jumping systems of time-delayed Chua’s circuit, *IEEE Trans. Syst. Man, Cybern.: Syst.*, **51** (2021), 2467–2475. <https://doi.org/10.1109/TSMC.2019.2914491>
20. X. M. Zhang, Q. L. Han, X. Ge, B. Ning, B. L. Zhang, Sampled-data control systems with non-uniform sampling: a survey of methods and trends, *Ann. Rev. Control*, **55** (2023), 70–91. <https://doi.org/10.1016/j.arcontrol.2023.03.004>

21. Y. Niu, K. Shi, X. Cai, S. Wen, Adaptive smooth sampled-data control for synchronization of T–S fuzzy reaction-diffusion neural networks with actuator saturation, *AIMS Math.*, **10** (2025), 1142–1161. <https://doi.org/10.3934/math.2025054>

22. Y. Wang, Y. Cao, Z. Guo, T. Huang, S. Wen, Event-based sliding-mode synchronization of delayed memristive neural networks via continuous/periodic sampling algorithm, *Appl. Math. Comput.*, **383** (2020), 125379. <https://doi.org/10.1016/j.amc.2020.125379>

23. X. Yang, T. Zhao, Q. Zhu, Aperiodic event-triggered controls for stochastic functional differential systems with sampled-data delayed output, *IEEE Trans. Automat. Control*, **70** (2025), 2090–2097. <https://doi.org/10.1109/TAC.2024.3486978>

24. E. Fridman, A refined input delay approach to sampled-data control, *Automatica*, **46** (2010), 421–427. <https://doi.org/10.1016/j.automatica.2009.11.017>

25. K. Liu, E. Fridman, Networked-based stabilization via discontinuous Lyapunov functionals, *Int. J. Robust Nonlinear Control*, **22** (2012), 420–436. <https://doi.org/10.1002/rnc.1704>

26. A. Seuret, C. Briat, Stability analysis of uncertain sampled-data systems with incremental delay using looped-functionals, *Automatica*, **55** (2015), 274–278. <https://doi.org/10.1016/j.automatica.2015.03.015>

27. X. Zhuang, Y. Tian, H. Wang, State estimation of networked nonlinear systems with aperiodic sampled delayed measurement, *ISA Trans.*, **156** (2025), 179–187. <https://doi.org/10.1016/j.isatra.2024.11.029>

28. X. Zhuang, H. Wang, Y. Tian, Delayed sampled impulsive observer design for a class of non-affine nonlinear systems with aperiodic sampled and delayed measurements, *Int. J. Robust Nonlinear Control*, **35** (2025), 3308–3316. <https://doi.org/10.1002/rnc.7842>

29. R. Zhang, X. Liu, D. Zeng, S. Zhong, K. Shi, A novel approach to stability and stabilization of fuzzy sampled-data Markovian chaotic systems, *Fuzzy Sets Syst.*, **344** (2018), 108–128. <https://doi.org/10.1016/j.fss.2017.12.010>

30. X. M. Zhang, Q. L. Han, A. Seuret, F. Gouaisbaut, An improved reciprocally convex inequality and an augmented Lyapunov–Krasovskii functional for stability of linear systems with time-varying delay, *Automatica*, **84** (2017), 221–226. <https://doi.org/10.1016/j.automatica.2017.04.048>

31. R. Zhang, D. Zeng, S. Zhong, Novel master–slave synchronization criteria of chaotic Lur'e systems with time delays using sampled-data control, *J. eFranklin Inst.*, **354** (2017), 4930–4954. <https://doi.org/10.1016/j.jfranklin.2017.05.008>

32. H. B. Zeng, K. L. Teo, Y. He, A new looped-functional for stability analysis of sampled-data systems, *Automatica*, **82** (2017), 328–331. <https://doi.org/10.1016/j.automatica.2017.04.051>

33. X. Zhuang, Y. Tian, H. A. Ghani, H. Wang, S. A. Ali, Sampled-data neural network observer for motion state estimation of full driving automation vehicle, *IEEE Trans. Veh. Technol.*, **74** (2025), 2726–2738. <https://doi.org/10.1109/TVT.2024.3479416>

34. K. Yu, Y. Li, Adaptive fuzzy control for nonlinear systems with sampled data and time-varying input delay, *AIMS Math.*, **5** (2020), 2307–2325. <https://doi.org/10.3934/math.2020153>

---

35. R. Datta, R. Saravanakumar, R. Dey, B. Bhattacharya, Further results on stability analysis of Takagi–Sugeno fuzzy time-delay systems via improved Lyapunov–Krasovskii functional, *AIMS Math.*, **7** (2022), 16464–16481. <https://doi.org/10.3934/math.2022901>

36. Z. Zhao, W. Lin, Extended dissipative analysis for memristive neural networks with two-delay components via a generalized delay-product-type Lyapunov–Krasovskii functional, *AIMS Math.*, **8** (2023), 30777–30789. <https://doi.org/10.3934/math.20231573>

37. A. Seuret, F. Gouaisbaut, Wirtinger-based integral inequality: application to time-delay systems, *Automatica*, **49** (2013), 2860–2866. <https://doi.org/10.1016/j.automatica.2013.05.030>

38. W. J. Lin, Y. He, M. Wu, Q. Liu, Reachable set estimation for Markovian jump neural networks with time-varying delay, *Neural Networks*, **108** (2018), 527–532. <https://doi.org/10.1016/j.neunet.2018.09.011>



AIMS Press

© 2025 the Author(s), licensee AIMS Press. This is an open access article distributed under the terms of the Creative Commons Attribution License (<https://creativecommons.org/licenses/by/4.0/>)